Polycyclic Aromatic Compounds, 26: 345–365, 2006

ISSN: 1040-6638 print / 1563-5333 online
DOI: 10.1080/10407780601028132

Taylor & Francis
Taylor & Francis Group

MOLECULAR GEOMETRY, *CYP1A* GENE INDUCTION AND CLASTOGENIC ACTIVITY OF CYCLOPENTA[*c*]PHENANTHRENE IN RAINBOW TROUT

Paweł Brzuzan
Łukasz Jurczyk
Maciej Woźny
Department of Environmental Biotechnology, University of Warmia and Mazury in Olsztyn, Olsztyn, Poland
Maciej Góra
Department of Organic Chemistry, Jagiellonian University, Krakow, Poland
Michał K. Łuczyński
Department of Chemistry, University of Warmia and Mazury in Olsztyn, Olsztyn, Poland
Henryk Kuźmiński
Department of the Salmonid Research in Rutki, Inland Fisheries Institute in Olsztyn, Poland
Wojciech Nitek
Department of Crystallography, Jagiellonian University, Krakow, Poland

Cyclopenta[c]phenanthrene (CP[c]Ph) is a PAH member that shows similarities to bay- and fjord region possessing PAHs. On the basis of X-ray measurements it was found that the molecule of this hydrocarbon is planar. In this case,

We thank Professor Miroslaw Luczyński, Department of Environmental Biotechnology, UWM in Olsztyn, and two anonymous reviewers for helpful comments on the paper; M.Sc. Elźbieta Ziomek for the collection and preparation of the blood smears; and M.Sc. Renata Lewandowska for her excellent technical assistance. This work was supported by the Polish Committee for Scientific Research, Project No. 2 P06D 001 29.

Address correspondence to Michał K. Łuczyński, Department of Chemistry, University of Warmia and Mazury in Olsztyn. Pl. Lodzki 4, 10-957 Olsztyn, Poland. E-mail: michalkl@uwm.edu.pl

intramolecular strains caused by repulsion between protons in the pseudo *fjord-region are balanced by both the shortening of some bonds which acquire more double bond character, and by the enlargement of exocyclic angles within the* pseudo *fjord-region. The activity of CP[*c*]Ph was investigated* in vivo *in rainbow trout,* Oncorhynchus mykiss. *The CYP1A mRNA levels following 48h-treatment with CP[*c*]Ph or benzo[*a*]pyrene (B[*a*]P; positive control) were determined and compared with incidences of clastogenic changes observed in the peripheral blood erythrocytes. We have found that the ability to induce* CYP1A *by these PAH compounds is positively correlated with the incidences of clastogenic changes in rainbow trout erythrocytes.*

Keywords clastogenic activity, crystal structure, cyclopenta[*c*]phenanthrene, CYP1A mRNA induction, polycyclic aromatic hydrocarbons, rainbow trout

INTRODUCTION

Polycyclic aromatic hydrocarbons (PAHs) are ubiquitous environmental agents and a wealth of studies have documented their carcinogenic, immunotoxic and endocrine disrupting effects (1). PAHs are formed in the process of incomplete combustion of organic material and are found, for example, in engine exhaust, cigarette smoke, soil, water and food. The carcinogenicity of PAHs is dependent on their metabolic activation—in three metabolic steps biologically inactive hydrocarbon may become an active carcinogen. Those three steps comprise the oxidation of the aromatic ring catalyzed by the P450 cytochrome system, the hydrolysis of the obtained epoxide, and the subsequent oxidation of bay-region or fjord-region double bond. Such a diol-epoxide is capable of covalent binding to the DNA and, as a consequence, causes a mutation and initiates cancer (2). Furthermore, some 4- or 5-ring PAHs, such as benzo[*a*]pyrene (B[*a*]P), are isosteric to sex steroids and are able to induce tumor formation in estrogen-responsive tissues such as the mammary gland, ovary, and uterus (3). The fact that compounds of diverse structure, such as B[*a*]P and its metabolites, have the ability to bind to the estrogen receptor (ER) isoforms (4, 5) resulted in concern that exposure to natural and synthetic PAH chemicals may adversely affect humans and animals.

The majority of PAH studies have examined mutagenicity, carcinogenicity and endocrine disrupting potential of B[*a*]P and its metabolites.

However, it is also necessary to determine the properties of other PAHs, which may be present in the environment. There are two important reasons for such studies: 1) frequent exposure of organisms to potential carcinogens, and 2) correlation between structure and biological activity of a given PAH. Cyclopenta[*a*]phenanthrene (CP[*a*]Ph) and its derivatives, for example, have been very well investigated, and their metabolites and carcinogenic properties have been described by Coombs and Bhatt (6). The structure of cyclopenta[*c*]phenanthrene (Figure 1), which might be considered as a bay region substituted phenanthrene derivative, suggests that the biological activity of both B[*a*]P and CP[*c*]Ph should be similar; certain bay-region PAHs, including B[*a*]P, exert their effects through the aryl hydrocarbon receptor (AhR), which is a ligand-activated transcription factor that regulates the activation of several genes that encode phase I (including genes encoding P4501A; *CYP1A*) and phase II drug metabolism enzymes in the liver (reviewed in 7). On the other hand, a recess in the CP[*c*]Ph molecule which is made up of three aromatic rings and terminal aliphatic ring may be considered a PAH with *pseudo* fjord-region. Although these compounds are metabolized to fjord-region *syn*- and *anti*-dihydrodiol epoxides (8), the interactions between the PAH structure and its biological activity remain unclear. For example, benzo[*c*]phenanthrene shows weak activity in a mouse skin painting test, but its metabolites, *syn*- and *anti*-dihydrodiol epoxides, are among the most potent carcinogens (8).

Surprisingly, little is known about the interactions of CP[*c*]Ph, and related compounds, in living organisms. To our knowledge, only Marrocchi et al. (9) have reported data on the mutagenic activity of CP[*c*]Ph and some of its derivatives, determined against *Salmonella typhimurium* strains in Ames test. Because no investigations have so far been conducted to assess biological activity of cyclopenta[*c*]phenathrenes in animals, we have begun a research program to study the effects of the

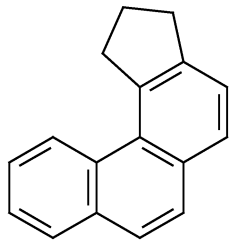

Cyclopenta[*c*]phenanthrene
CP[*c*]Ph

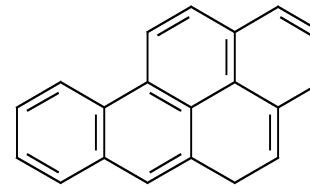

Benzo[*a*]pyrene
B[*a*]P

FIGURE 1. Chemical structures of CP[*c*]Ph and B[*a*]P.

CP[*c*]Ph in rainbow trout (*Oncorhynchus mykiss*). In the present work, the effects of CP[*c*]Ph on both, the AhR-regulated CYP1A gene expression and clastogenic changes in peripheral blood erythrocytes of rainbow trout have been investigated. We exposed fish to CP[*c*]Ph and B[*a*]P (positive control) for 48 h to evaluate and compare the effects of either PAH on CYP1A mRNA levels in liver (site of metabolic activation) and head kidney (blood forming tissue). Then, we related the CYP1A gene expression levels of either tissue of each individual fish with the respective frequency of observed nuclear lesions in peripheral blood erythrocytes, determined by nuclear abnormalities test and comet assay. Our results show that though a planar PAH compound, CP[*c*]Ph is less potent at inducing CYP1A gene expression than B[*a*]P; for either PAH, the liver showed greater induction potential than head kidney. Moreover, the ability to induce *CYP1A* by these PAH compounds appears to be positively correlated with the incidences of clastogenic changes in rainbow trout erythrocytes. We conclude that exposure to the two polycyclic aromatic hydrocarbons (CP[*c*]Ph and B[a]P) would be expected to elicit similar phase I biotransformation reactions in rainbow trout.

MATERIALS AND METHODS

Synthesis of 2,3-dihydro-1*H*-cyclopenta[*c*]phenanthrene

^{1}H and ^{13}C NMR spectra were obtained with Bruker AMX500 spectrometer at 500 and 125 MHz respectively. IR and MS spectra were obtained with Bruker IFS 40 as KBr pellets and HP 5971A mass selective detector at 70 eV. Elemental analysis was done on EA 2000 Elemental Analyser.

The pure CP[*c*]Ph was prepared as follows:
An ethanolic solution of 5-amino-2,3-dihydro-1*H*-cyclopenta[*c*] phenanthrene-4-aminonitrile (10) was heated in an autoclave at 220°C for 3 hrs and after usual workup the 5-amino-2,3-dihydro-1*H*-cyclopenta [*c*]phenanthrene (mp. 128–129°C) was isolated in 83% yield. The spectroscopic data for amine were as follows: **IR** (KBr) ν [cm^{-1}]: 3447, 3367, 3049, 2952, 2909, 1628, 1592, 1527, 1429, 813, 749. **^{1}H NMR** ($CDCl_3$) δ [ppm]: 2.22 (quint, 2H, $J = 7.4$ Hz); 3.06 (t, 2H, $J = 7.5$ Hz); 3.69 (t, 2H, $J = 7.4$ Hz), 4.07 (br-s, 2H), 6.94 (s, 1H), 7.55–7.61 (m, 2H), 7.65 (d, 1H, $J = 7.5$ Hz), 7.78 (d, 1H, $J = 7.5$ Hz), 7.87 (dd, 1H, $J = 7.85$ Hz; $J = 1.5$ Hz), 8.80 (d, 1H, $J = 8.5$ Hz). **^{13}C NMR** ($CDCl_3$) δ [ppm]: 25.71, 33.45, 37.22, 109.67, 120.32, 120.56, 124.94, 125.56, 125.86, 127.04, 128.21, 129.18, 130.43, 131.84, 133.14, 141.51, 144.55. Elemental analyse for $C_{17}H_{15}N$ (M = 233.31). Required:

87.52% C, 6.48% H, 6.00% N; found: 87.73% C, 6.58% H, 5.97% N. To the well stirred suspension of the 5-amino-2,3-dihydro-1*H*-cyclopenta[*c*]phenanthrene (160 mg; 0.69 mmol) in ice-cold concentrated hydrochloric acid (0.6 ml) diluted with water (1.0 ml) solution of sodium nitrite (50.0 mg; 0.73 mmol) in 0.5 ml of cold water was added dropwise at 2–5°C. After 1 h of additional stirring hypophosphorous acid (8.0 mmol; 1.6 ml of 30% H_3PO_2 inwater solution) was added. The mixture was then allowed to stand overnight in a refrigerator. After the addition of sodium hydroxide (200 mg; 5.0 mmol) in 3 mL of water the mixture was extracted with CH_2Cl_2 (3 × 20 ml). Collected organic layers were combined and dried over magnesium sulphate. The solvent was removed under reduced pressure and the residue, after column chromatography (SiO_2/toluene), yielded crude 2,3-dihydro-1*H*-cyclopenta[*c*]phenanthrene (54 mg; 36%) which was crystallized from methanol-acetone solution (1:1; v/v). MS and NMR spectra of the hydrocarbon were in agreement with those described by Gacs-Baitz et al. (11). X-ray diffraction intensity measurement at room temperature (293 K) was carried out on a Kappa CCD (Enraf-Nonius) diffractometer equipped with a molybdenum X-ray tube and Oxford Cryostream cooler. The phase problem was solved using the SHELXS-97 (12) program and the refinement was performed with SHELXL-97 (13). Details of the measurement and refinement are available on request. Benzo[*a*]pyrene was purchased from Fluka (Buchs, Switzerland).

Fish Handling and Sampling

The fish were treated in accordance with the rules approved by the Local Ethical Commission No. 38/N issued on 29.07.2004 (conforming to principles of Laboratory Animal Care, NIH publication No. 86–23, revised in 1985). Juvenile rainbow trout (38 g mean weight, 15 cm mean length) were held at the Department of Salmonid Research in Rutki, Inland Fisheries Institute in Olsztyn, Poland. Fish were individually tagged with passive integrated transponders (PIT) which allowed further automated data acquisition using data-entry station (14). The fish were acclimatised for two weeks at 7°C. For the gene induction study, individuals were randomly sampled, anesthetized using a dose (0.5 ml/l) of 2% Etomidate to avoid animal suffering, and injected intraperitoneally with either B[*a*]P (positive control) or CP[*c*]Ph dissolved in corn oil at doses of 10 mg/kg body weight, or with corn oil alone (Control O). A single group of experimental fish was injected with B[*a*]P at a dose of 50 mg/kg body weight. One group (Control) consisted of fish that were untreated. Fish were placed in an 800 l flow-through tank (well water, 600 l/h) for

48 h at 7°C. At the end of the experiment, the length and weight of all fish were recorded. Then, 5 random fish from each PIT-identified group were anesthetized and a portion (1 ml) of peripheral blood was collected from each fish to examine the nuclear abnormalities in erythrocytes and for the comet assay. The fish were then sacrificed, and the tissues (liver and head kidney) were immediately stored in RNA *Later*^{TM} at −20°C (Qiagen, Hilden, Germany).

Nuclear Abnormalities (NA) Test

Several types of variations from the usual erythrocyte nucleus morphology were observed following the fish exposure to a PAH contaminant. Following Carrasco et al. (15), the nuclear abnormalities can be classified into five categories. *Micronuclei* are non-refractory structures, of the same color as the nucleus and with a round, almond or ovoid shape about one-fifth the size of the main nucleus; "*blebbed*" nuclei present a relatively small evagination (bleb) of the nuclear envelope which seem to contain euchromatin; "*lobed*" nuclei are those with evaginations larger than the blebs described above; "*notched*" nuclei present an appreciable depth into a nucleus that does not contain nuclear material; and "*vacuolated*" nuclei are those with a well-defined hole devoid of any visible material.

For the *NA* test about 200 μl of peripheral blood was smeared onto a microscope slide and allowed to dry for a few minutes. After that the slides were fixed in methanol for 10 minutes, air dried and stained with 10% Giemsa. Then the samples were washed in distilled water for 20 minutes. From each animal, 1000 erythrocytes were scored under 1000× magnification, to determine the frequency of particular nuclear lesions. In order to take into account the possible heterogeneity of the smear, several fields in topographically separated areas of the slide were chosen.

Measurement of DNA Strand Breakage by Single Cell Gel Electrophoresis (Comet Assay)

Comet assay was conducted on peripheral blood erythrocytes as described by Woźnicki et al. (16), with slight modifications. Frosted slides were precoated with 1% agarose (normal melting agarose; NMA) in PBS. After the agarose had solidified, a suspension of erythrocytes was prepared by adding PBS to obtain 1–2 × 10^4 cells per slide (6–7 × 10^5 cells/ml).

Single cell suspension was mixed with 65 μl of 0.5% agarose (low melting agarose; LMA) and placed on the first agarose layer. A coverslip

was added and agarose was allowed to solidify for 10 minutes on ice. After removing the coverslip, the third layer of 0.5% LMA agarose was added and left to solidify on ice. The coverslip was removed and the cells were lysed in freshly made lysing solution (2.5 M NaCl, 100 mM EDTA, 10 mM Tris·HCl, 1% sodium sarcosinate, 1% Triton X-100 and 10% DMSO, pH = 10.0) for 1 h at 4°C. After lysis of the cells, the slides were placed on the horizontal gel box and covered with cold (about 4°C) alkaline buffer (10 N NaOH and 200 mM EDTA, pH = 12.3). The slides were left in the alkaline buffer for 20 minutes to allow for the unwinding of DNA. Slides were electrophoresed at 25 V and 300 mA for 15 minutes. After electrophoresis, the slides were neutralized three times for 5 minutes with the cold (4°C) neutralization buffer (0.4 M Tris·HCl, pH = 7.5), stained with 20 μg/ml ethidium bromide and examined on the same day using a Nikon Optiphot 2 epifluorescence microscope.

For each animal, 100 cells per slide (300 per experimental group) were visually scored at random for the empirical score of damage they exhibited. The damage categories were estimated according to the approximate percentage DNA in comet's tail as described by Gedik et al. (17). As a positive control, a sample with 250 μM H_2O_2 was used. Cell viability of control animals evaluated by 5–6 carboxyfluorescein diacetate (CFDA) with ethidium bromide ranged from 98% to 100%; the test was done to make sure that the procedure of cell isolation did not damage the cells (18).

Total RNA Isolation and Semi-Quantitative RT-PCR

RNA*Later*™ preserved tissues were homogenized and extracted for total RNA isolation using Fenzol Reagent (A&A Biotechnology, Gdynia, Poland) according to the manufacturer's protocol. Then RNA extract was re-suspended in 100 μl of diethylpyrocarbonate treated water (DEPC-H_2O). RNA samples were incubated at 37°C for 30 minutes with RNase-free DNase I (Promega, Madison, WI, USA) to ensure that genomic DNA was not amplified during PCR, and quantified using a Bio*Photometer* (Eppendorf, Hamburg, Germany). At first, strand cDNA was synthesized using oligo$(dT)_{18}$ primer (Fermentas, Burlington, Canada) according to the manufacturer's protocol and used in RT-PCR with the primer pairs specific to target gene (*CYP1A*) in rainbow trout (Table 1). Standard PCR reaction conditions and thermal cycling protocol were described in the papers cited in Table 1. In order to adopt a more semi-quantitative approach for analysis of the gene expression, both CYP1A and ß-actin gene (external standard) were amplified using a series of cycle numbers

TABLE 1. Gene-Specific Forward and Reverse Primer Sequences

Target gene	Accession ID[a]	Direction	5′-3′ Primer sequence	Amplicon (bp)
CYP1A (19)	AF361643	Forward	CTG TCT TGG GCC GTT GTG TAC CTT GTG	208
		Reverse	TAT CCT TGA TCG TGC AGT GTG GGA TGG	
$\beta-$actin[b]	AF254414	Forward	GAG CGT AGC CCT CGT AGA TGG GTA CTG TGT	252
		Reverse	ATC ACA CCT TCT ACA ACG AGC TGA GGG TGG	

CYP1A, cytochrome P4501A protein; β-actin, β-actin protein.
[a]NCBI gene bank accession ID, as confirmed by BLAST sequence analysis.
[b]This study.

(20–30). Following this procedure the optimal cycle number was determined and subsequently employed in the expression studies. If ß-actin fragment amplification was equal across all samples, it was concluded that any difference in mRNA levels in the corresponding samples was due to individual variation and not to experimental error imposed by RNA loading. Gene expression levels determined by densitometric analyses (KODAK Gel Logic 200 Imaging System) were then given as the ratio of the gene of interest (nominator) versus a stably expressed housekeeping gene (ß-actin, denominator). These target gene / ß-actin ratios were then expressed as relative arbitrary units (R.A.U.; means $\pm$ SD, $n = 5$) with a value of 100 for the respective control groups.

Statistical Analyses

Homogeneity of the experimental groups for length and weight were tested with one-way ANOVAs. The frequencies of micronuclei and other nuclear lesions were expressed per 1000 cells (‰). The nuclear abnormalities other than micronuclei were considered together for statistical analysis in the absence of evidence or suggestions of differences in their origin. Micronuclei, the standard indicators of genotoxicity, were always considered separately from the other nuclear abnormalities. A Kruskal-Wallis test was used to compare the frequency of nuclear abnormalities between the control and treatment groups. A posteriori Mann-Whitney test was employed.

The results of the comet assay for each experimental group were expressed as the averages and standard deviations ($n = 300$ cells). Statistical analysis of the differences between samples was performed using the Kruskal-Wallis test. The R.A.U. means of the target genes were compared using Kruskal-Wallis test and a posteriori Mann-Whitney test.

Finally, direct correlations (r_s values) among the respective target gene expression levels and nuclear lesions scored within individual fish were performed using Spearman rank correlation test. Levels of significance were adjusted according to Miller method (20), by dividing the significance level by the number of tests performed on the same data set. In this study, the critical level of significance was set by dividing the standard significance level ($P = 0.05$) by four, the number of nuclear abnormalities data tested against each individual R.A.U. value for respective genes. This method yielded a critical significance level (P) of 0.0125 for each correlation performed. All analyses were carried out using the STATISTICA 6.0 package.

RESULTS

Structure of 2,3-dihydro-1*H*-cyclopenta[*c*]phenanthrene

Crystals of Cp[*c*]Ph were obtained by dissolving crude 2,3-dihydro-1*H*-cyclopenta[*c*]phenanthrene (53 mg) in 1 ml of hot methanol and acetone (1:1; v/v) mixture. The solution was allowed to stand overnight at room temperature. Crystals of pure Cp[c]Ph were filtered off, washed with ice-cold methanol (1 ml) and dried on air.

Crystal data and structure refinement for Cp[c]Ph were as follows: Empirical formula: C17 H14; Formula weight: 218.28; Temperature: 293(2) K; Wavelength: 0.71070 Å; Crystal system: monoclinic; Space group: P2; Unit cell dimensions: a = 9.4790(3) Å, $\alpha = 90^\circ$, b = 10.1960(3) Å, $\beta = 94.883(2)^\circ$, c = 12.0020(5) Å, $\gamma = 90^\circ$; Volume: 1155.76(7) $Å^3$; Z = 4; Density (calculated): 1.254 Mg/m^3; Absorption coefficient: 0.071 mm^{-1}; F(000) 464; Theta range for data collection: 3.30 to 26.75°; Index ranges: $0 <= h <= 11, 0 <= k <= 12, -15 <= l <= 15$; Reflections collected: 2445; Independent reflections: 2445 [R(int) = 0.0000]; Completeness to theta = 26.75°: 99.8%; Absorption correction: none; Refinement method: full-matrix least-squares on F^2; Data/restraints/parameters: 2445/0/154; Goodness-of-fit on F^2: 1.056; Largest difference peak and hole: 0.258 and −0.230 e.$Å^{-2}$; Final R indices [I > 2sigma(I)]: R1 = 0.0720, wR2 = 0.1690; R indices (all data): R1 = 0.1334, wR2 = 0.2165.

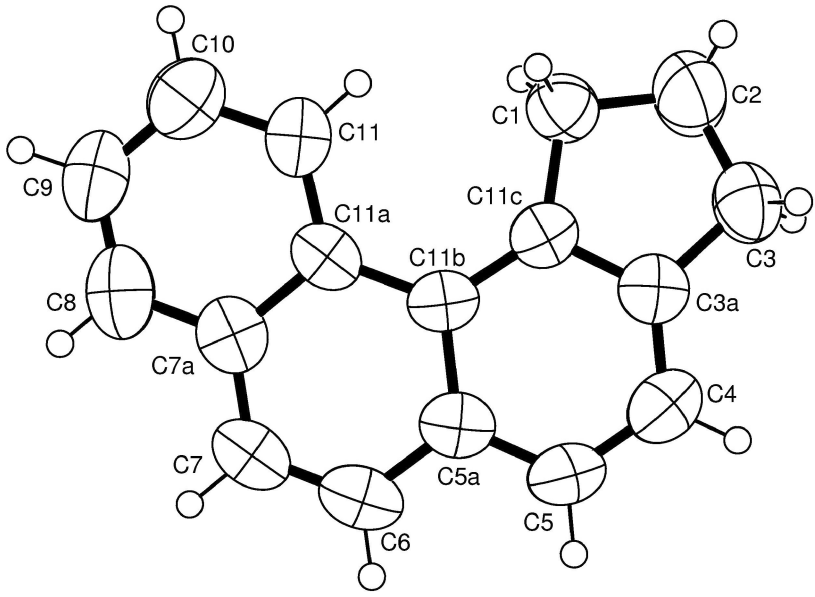

FIGURE 2. ORTEP (3) projections of asymmetric units of CP[*c*]Ph. The atomic displacement ellipsoids are on 50% probability level.

The asymmetric unit of the unit cell determined at room and low temperature consists of one molecule of CP[*c*]Ph [ORTEP [21] drawing shown in Figure 2], with bond lengths and bond angles listed in Table 2. The torsion angles (Table 2) showed that the whole molecule was approximately planar. The most striking feature of the molecular shape is the planarity of the *pseudo* fjord-region, demonstrated by the

TABLE 2. Selected Angles and Bond Lengths Describing CP[*c*]Ph Geometry

Torsion angles [°]	
C(1)-C(11C)-C(11A)-C(11)	−4.2(2)
C(1)-C(11C)-C(11B)-C(11A)	−0.8(4)
C(11C)-C(11B)-C(11A)-C(11)	−4.3(4)
Angles [°]	
C(1)-C(11C)-C(11B)	131.5(2)
C(11)-C(11A)-C(11B)	123.9(2)
C(11A)-C(11B)-C(11C)	126.0(2)
Distance [Å]	
C(7)-C(6)	1.373(4)

torsion angle C11-C11A-C11B-C11C = −4.3(4)°. However, the large exocyclic angles C11-C11A-C11B and C11A-C11B-C11C (123,9° and 126,0° respectively) reveal a strong interaction between protons H(1) and H(11).

It was already established that the occurrence of small alkyl (electron-donating) group in bay-region gives rise to carcinogenicity in cyclopenta [*a*]phenanthrene series due to the easier metabolic formation of bay-region *anti*-dihydrodiol epoxides (6). In the case of Cp[*c*]Ph fused alicyclic moiety might be considered as two electron-releasing alkyl groups at C3 and C4 in the parent phenanthrene skeleton which correspond to C11 and C12 substitution in cyclopenta[*a*]phenanthrene.

A search in the Cambridge Structural Data Base (CSDB) was performed to compare Cp[*c*]Ph geometry with other phenanthrene derivatives substituted at C(11C). The fragments containing electronwithdrawing substituents like $-NO_2$ and –COOH groups as well as polyaromatics were rejected manually. Also, data concerning 4-methylphenathrene was rejected as unreliable. After such a selection only six crystal structures containing nine fragments were left. Those were: benzo[*c*]phenanthrene (22–24), 1-Methyl-phenanthro(3,4-*b*)thiophene (25), 1-phenanthryl-methanol (26), 1,4-dimethylbenzo[*c*]phenanthrene (24). All those molecules are strongly twisted. The torsion angles correspond with C(11)-C(11A)-C(11C)-C(1) at Cp[*c*]Ph, which is a measure of twisting, varying in the range of −39.77 to – 31.00° with a mean of absolute values 29.58°. The mean values of angles equivalent to C(1)-C(11C)-C(11B), C(11)-C(11A)-C(11B) and C(11)-C(11A)-C(11B) adopts values 125.30°, 123.96° and 124.87° respectively. Distance C(7)-C(6) varies in a very narrow range of 1.33–1.36 Å with a mean value 1.34 Å. This suggests that the bond has a double rather than an aromatic character.

In the case of CP[*c*]Ph, the torsion angle C(1)-C(11C)-C(11A)-C(11) is close to 0° value and the whole molecule is approximately flat. Angles C(1)-C(11C)-C(11B), C(11)-C(11A)-C(11B) and C(11)-C(11A)-C(11B) are similar to the values retrieved from CSDB. The distance C(7)-C(6) is slightly but significantly longer than that mentioned above and has a more aromatic character. It may be a result of the molecule flatness.

Induction of Nuclear Abnormalities and DNA Strand Breakage

Table 3 shows the averages and standard deviations of lengths and weights for the group of fish used in this work. No significant differences among experimental groups were found using single-factor ANOVAs ($F_w = 1.639$, $P = 0.170$; $F_l = 2.172$, $P = 0.083$, for weight and length, respectively). The results of the experimental induction of

TABLE 3. Biological Characteristics of Fish Tested

		Total weight (grams)		Total length (centimeters)	
Experimental group	*N*	Mean	SD	Mean	SD
Control	15	39.5	0.1	15.6	0.2
Control O	13	39.3	6.0	15.3	0.7
B[*a*]P-10	11	36.8	0.6	15.1	0.1
CP[*c*]Ph-10	14	36.1	6.8	15.1	0.9
B[*a*]P-50	12	40.3	0.9	15.4	0.1

Weight and length averages and standard deviations of the fish used for each experimental group. *N*, number of animals analyzed; SD, standard deviation.

micronuclei and other nuclear abnormalities are presented in Table 4. There were no differences between the untreated fish (Control) and those injected with corn oil only (Control O) in respect to either nuclear abnormalities or comet assay. Neither notched nuclei nor micronuclei were observed in blood samples taken from the control and experimental groups, except for one micronucleus which was found in the sample from a fish injected with B[*a*]P-50. Significant differences between all the experimental groups were found, however, for other nuclear lesions and comet cells using Kruskall Wallis tests ($P = 0.0013$ and $P = 0.0430$, respectively). Trouts injected with both doses of B[*a*]P, 10- and 50 mg/kg body weight, showed a significant increase of the nuclear abnormalities ($p < 0.01$) in comparison to the control groups. The effect of treatment with CP[*c*]Ph-10 on the frequency of nuclear abnormalities in the erythrocytes of rainbow trout was not significant. The fish treated with CP[*c*]Ph and B[*a*]P (but not those with B[*a*]P-10) showed an increased frequency of comet cells ($p < 0.05$) with respect to controls.

Expression of *CYP1A*

The basal expressions of *CYP1A* in liver and in head kidney tissue were confirmed by RT-PCR (Figure 3), where specific bands of expected PCR products' size were observed for CYP1A. Equal ß-actin amplification across all samples indicated that mRNA were all intact. No products were amplified in negative controls which contained water instead of cDNA, and no products were amplified when genomic DNA was used as a template. By reducing the cycle number from 30 to 20 it was possible to select a cycle number producing clear bands: in the case of liver and head kidney tissue the number of cycles was 24 for ß-actin and 28 for

TABLE 4. Frequencies (Averages and Standard Deviations (±SD)) of Nuclear Abnormalities (Expressed per 1000 cells) and Comet Cells (Expressed per 300) in Peripheral Blood Erythrocytes of Rainbow Trout Treated with Different Compounds. K-W: Kruskall Wallis Test

	Nuclear abnormality					
Experimental group	Micronuclei (M)	Blebbed (B)	Lobed (L)	Vacuolated (V)	B-L-V K-W ($P = 0.0013$)	Comet K-W ($P = 0.0430$)
Control	0 (±0)	0 (±0)	0 (±0)	0 (±0)	0 (±0)	1.33 (±1.53)
Control O	0 (±0)	0 (±0)	0 (±0)	0 (±0)	0 (±0)	1.33 (±0.58)
B[*a*]P-10	0 (±0)	2.00 (±1.00)	0 (±0)	1.00 (±1.73)	3.00 (±2.45)**	3.00 (±2.00)
CP[*c*]Ph-10	0 (±0)	0.40 (±0.54)	0.60 (±0.89)	2.20 (±2.49)	3.20 (±3.63)	4.00 (±1.00)*
B[*a*]P-50	0.20 (±0.45)	3.80 (±1.79)	2.00 (±1.87)	1.40 (±1.52)	7.20 (±2.30)**	3.67 (±1.15)*

B-L-V: the sum of blebbed, lobed and vacuolated nuclei. Statistical differences of the treated groups versus control groups: * $P < 0.05$; ** $P < 0.01$.

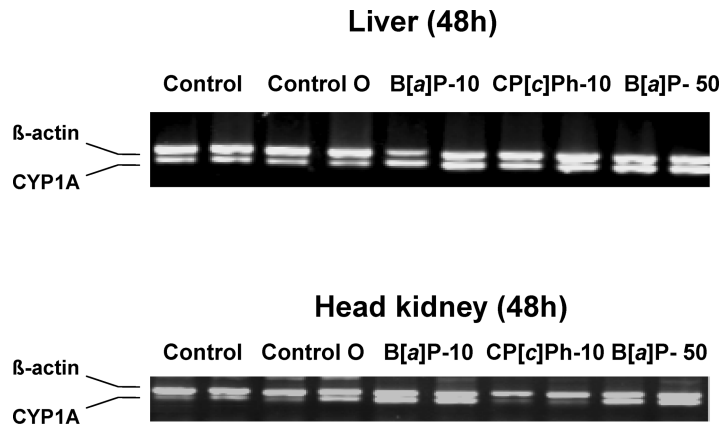

FIGURE 3. Representative RT-PCR gel electrophoresis results for liver and head kidney tissues of control and treated rainbow trout after a 48 h exposure. Expression of CYP1A mRNA normalized to the ß-actin internal control was assayed using semi-quantitative RT-PCR as described under "Materials and Methods." Data are presented for two representative fish from each experimental group. The signals exhibited the expected PCR product sizes and molecular masses, as previously described (19).

CYP1A, (data not shown). When a cycle number was fewer than 24, no products could be visualized for any gene. The mean control CYP1A mRNA levels were higher ($P = 0.009$) in liver (R.A.U. = 100) than those in head kidney (R.A.U. = 70), as determined by densitometric analyses on the gels (Figure 3).

Effects of B[*a*]P and CP[*c*]Ph on the Expression of *CYP1A*

The changes in CYP1A mRNA levels at 48 h upon xenobiotic exposure versus control groups were significant in liver ($P = 0.003$) and in head kidney ($P = 0.003$) (Figure 4). In the presence of B[*a*]P-10 and B[*a*]P-50 the expression of *CYP1A* was up-regulated in both tissues ($p < 0.01$), however, no B[*a*]P concentration-dependent expression of *CYP1A* was observed. CP[*c*]Ph-10 induced *CYP1A* in liver ($p < 0.01$), but a decrease in CYP1A versus controls was observed in head kidney ($p < 0.05$). In both tissues, B[*a*]P-10 and B[*a*]P-50 were stronger inducers as compared to CP[*c*]Ph-10, with the mean induction levels of 2.3, 2.4, and 1.6-fold, respectively in liver ($p < 0.01$), and of 1.7, 1.4 and 0.8, respectively in head kidney ($p < 0.01$) (Figure 4).

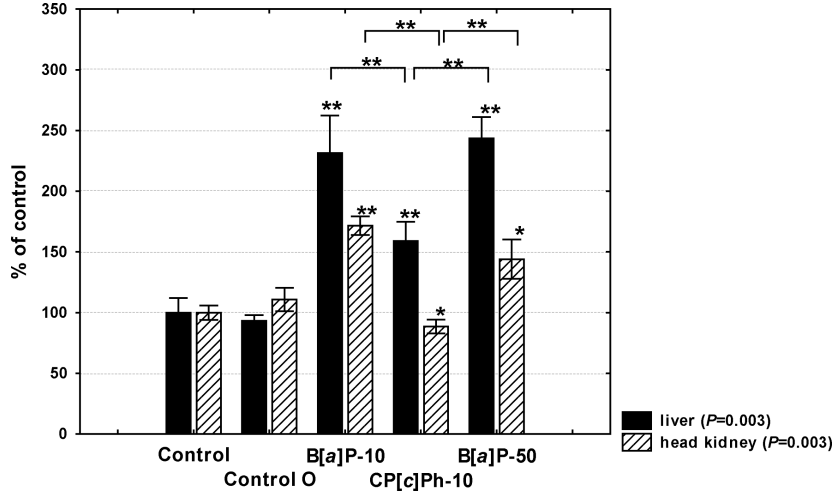

FIGURE 4. Expression of CYP1A mRNA in liver and head kidney tissues of control and treated rainbow trout after a 48 h exposure. The expression of CYP1A mRNA normalized to the ß-actin internal control was assayed using semi-quantitative RT-PCR as described under "Materials and Methods." Data shown were relative arbitrary units (R.A.U.; means ± SD, $n = 5$) with a value of 100 for the respective control groups (Control). Kruskal-Wallis test analyses to compare R.A.U. means between control and treatment groups were given for either tissue. Statistical differences of the treated groups with respect to control groups (Control), as well as within the treated groups were shown at top of the bars (Mann-Whitney $^{*}P < 0.05$; $^{**}P < 0.01$).

Relationships Between mRNA Expression Levels of CYP1A of Individual Fish and the Respective Frequency of Observed Nuclear Lesions

The frequencies of single or combined nuclear abnormalities and CYP1A mRNA expression levels were significantly correlated in individual fish over the entire data set (Table 5). Significant positive correlations ($P <$ adjusted critical significance level of 0.0125) were found between individual *CYP1A* expression level in liver ($r_s = 0.87$) and head kidney ($r_s = 0.67$) and the corresponding frequencies of the blebbed nuclei. A combined data analysis of the frequency of nuclear lesions showed a significant correlation with *CYP1A* expression levels in liver ($r_s = 0.80$), but was not significantly correlated with CYP1A mRNA levels in head kidney ($r_s = 0.42$) (Table 5).

TABLE 5. Correlation Coefficients, r_s (Spearman Rank Correlation Test) between the mRNA Expression Levels of CYP1A (R.A.U. Values) of Individual Fish and the Respective Frequency of Observed Nuclear Abnormalities

	Micronuclei (M)	Blebbed (B)	Lobed (L)	Vacuolated (V)	Combined lesions (M-B-L-V)
$CYP1A_{\text{LIVER}}$	0.17	0.87*	0.36	0.42	0.80*
$CYP1A_{\text{HEADKIDNEY}}$	0.08	0.67*	0.05	0.04	0.43

*Denotes a significant correlation at $p < 0.0125$.

DISCUSSION

It is most probable that steric hindrance and shape of the PAH molecule causes differences in activity between bay-region and fjord region hydrocarbons. In cyclopenta[*a*]phenanthrene series substitution in bay-region results in deformation of the molecule planarity and as a consequence causes easier access to the terminal aromatic ring. In contrast, introduction of the methyl group into the fjord-region of non-planar benzo[*c*]phenanthrene leads to the significant decreasing of its mutagenic potency. This can be rationalized by different biotransformation rates of the bay- and fjord region PAHs resulting in formation of mixture of metabolites, where the amount of harmful diolepoxides depends on the structure of the compound. It seems that the formation of such diolepoxides is roughly correlated with accessibility of the terminal aromatic ring to the cytochrome P450 oxidizing systems (24).

Crystallographic data showed that interactions between protons H(1) and H(11) in *pseudo* fjord-region of cyclopenta[*c*]phenanthrene result in some molecule geometry changes as compared to other phenanthrene derivatives. In cyclopenta[*a*]phenanthrenes an introduction of alkyl group into the bay-region twists ring A out of the plane (6). On the other hand fjord-region PAHs are twisted even having no substituents in the recess of the molecule. We expected a similar effect in the case of CP[*c*]Ph but, rather surprisingly, we have found that planarity of the molecule of this hydrocarbon is saved. In this case intramolecular strains caused by repulsion between protons in *pseudo* fjord-region are balanced by shortening some bonds which acquire more double bond character and by enlarging exocyclic angles within *pseudo* fjord-region (Table 2). It should be noted that these angles and bond lengths were comparable to those in bay-region of muta- and carcinogenic cyclopenta[*a*]phenanthrene derivatives (27). For example:

1,11-methano-15,16-dihydrocyclopenta[*a*]phenanthren-17-one which is planar but severing bond angle distortions possess an Iball index = 16 (28).

Certain PAHs, including B[*a*]P, exhibit high binding affinity for the aryl hydrocarbon receptor (29). AhR is a ligand-activated member of transcription factors that regulates the expression of multiple genes encoding members of the cytochrome P450 family, such as *CYP1A*. Varying responses of *CYP1A* may reflect a different potency of the AhR-ligand complex to alter the gene transcription rate. In the present study we confirmed the findings with B[*a*]P, but also we have found that CP[*c*]Ph induced the expression of *CYP1A*. Our results suggest also that B[*a*]P-10 or -50 are more potent than CP[*c*]Ph-10 at inducing *CYP1A,* this however needs to be proved in future by performing an electrophoretic mobility shift assay (EMSA). Nonetheless, these differences in potencies correlate with the reported genotoxic and mutagenic potentials for B[*a*]P and cyclopenta[*c*, *d*]pyrene, another cyclopenta-PAH (CP-PAH) species (30). In most genotoxicity tests in mammals (using isolated microsomes) DNA-damaging potentials of B[*a*]P were bigger than those of CP-PAH (31).

Interestingly, different tissue-specific levels of CYP1A mRNA expression were observed upon CP[*c*]Ph treatment. Whereas CP[*c*]Ph induced *CYP1A* in liver, with the mean induction level of 1.6-fold as compared to controls, the induction level in the head kidney was lower (0.8-fold) than in control groups. There are several hypotheses explaining why the head kidney was not as induced by CP[*c*]Ph as it was in the liver. We found in the study that constitutively the head kidney of rainbow trout may have much less CYP1A than their liver has. Because of lower levels of CYP1A it may be harder to detect induction with a moderately potent AhR-agonist such as CP[*c*]Ph. Another explanation could be that the number of AhR molecules present in the liver, and thus a potential to induce CYP1A genes, is higher compared to that in the head kidney. Furthermore, differentiated tissue expression upon CP[*c*]Ph exposure may also suggest that besides AhR there are other factors which could mediate CP[*c*]Ph responses in rainbow trout.

Greater CYP induction following the PAH exposure results in a higher biotransformation rate of the compound and accumulation of activated electrophilic metabolites (32, 33). The most common genotoxic effects exerted by these reactive compounds are DNA-adducts, which are responsible for the chromosome damage and subsequent formation of micronuclei and other nuclear abnormalities (34). Therefore, we examined the effects of CP[*c*]Ph on the peripheral blood erythrocytes of rainbow trout and compared them with those exerted by B[*a*]P, whose clastogenic

activity is well proved (35). In this work B[*a*]P at two doses, 10- and 50mg/kg of body weight, significantly increased the frequency of the nuclear abnormalities, whereas CP[*c*]Ph did not (Table 4). Moreover, a significant positive correlation found between the individual CYP1A gene expression levels in either liver or head kidney and the corresponding frequencies of blebbed erythrocytes (Table 5) is of importance, because it may suggest that the clastogenic effects in rainbow trout caused by the PAHs were determined by their ability to bind to AhR and induce CYP1A gene (Figure 3). We hypothesize that more numerous molecules of P4501A isozymes in rainbow trouts exposed to B[*a*]P biotransformed the compound at a higher rate than did fewer molecules of P4501A of fish treated with CP[*c*]Ph. The results of our studies in rainbow trout are consistent with results in other animal models (36, 37) where B[*a*]P induced CYP1A1 activity was found to be at a higher rate than less potent PAH's (i.e. CP[*c*]Ph).

In conclusion, clastogenic effects and CYP1A induction in response to CP[*c*]Ph or B[*a*]P exposure were investigated in rainbow trout. The fact that exposure to these xenobiotics increased the levels of CYP1A in liver and head kidney, corroborated an AhR-dependent gene regulation pathway, with B[*a*]P-10 or -50 being likely more potent at inducing the gene than CP[*c*]Ph-10. Furthermore, the ability of these AhR agonists to induce *CYP1A* was predictive of incidences of clastogenic changes in rainbow trout erythrocytes. We conclude that exposure to two polycyclic aromatic hydrocarbons (CP[*c*]Ph and B[a]P) would be expected to elicit similar phase I biotransformation reactions in *Oncorhynchus mykiss*, the teleost fish.

REFERENCES

1. J. F. Payne, A. Mathieu, and T. K. Collier, Ecotoxicological studies focusing on marine and freshwater fish. In: Dauben, P. E. T. (ed.), *PAHs—An Ecotoxicological Perspective*. West Sussex, UK: Wiley (2003).
2. M. E. Burczynski, and T. M. Penning, Genotoxic polycyclic aromatic hydrocarbon ortho-quinones generated by aldo-keto reductases induce CYP1A1 via nuclear translocation of the aryl hydrocarbon receptor. *Cancer Res.* 60 (2000):908–915.
3. K. C. Fertuck, J. B. Matthews, and T. R. Zacharewski, Hydroxylated benzo[*a*]pyrene metabolites are responsible for in vitro estrogen receptor-mediated gene expression induced by benzo[*a*]pyrene, but do not elicit uterotrophic effects in vivo. *Toxicol. Sci.* 59 (2001):231–240.
4. A. M. Brzozowski, A. C. W. Pike, Z. Deuter, R. E. Hubbard, T. Bonn, O. Engstrom, L. Ohman, G. L. Green, J.-A. Gustafsson, and M. Carlquist, Molecular basis for agonism and antagonism in the oestrogen receptor. *Nature* 389 (1997):753–758.

5. A. C. W. Pike, A. M. Brzozowski, R. E. Hubbard, T. Bonn, A.-G. Thorssel, O. Engstrom, J. Ljunggren, J.-A. Gustafsson, and M. Carlquist, Structure of the ligand-binding domain of oestrogen receptor β in the presence of partial agonist and a full antagonist. *Embo Journal* 18 (1999):4608–4618.
6. M. M. Coombs and T. S. Bhatt, Cyclopenta[*a*]phenanthrenes. Cambridge: Cambridge Monographs on Cancer Research, (1987).
7. J. C. Rowlands, and J. A. Gustafsson, Aryl hydrocarbon receptor-mediated signal transduction. *Crit. Rev. Toxicol.* 27 (1997):109–134.
8. H. J. Einolf, S. Amin, H. Yagi, D. M. Jerina, and W. M. Baird, Benzo[*c*]phenanthrene is activated to DNA-binding diol epoxides in the human mammary carcinoma cell line MCF-7 but only limited activation occurs in mouse skin. *Carcinogenesis* 17 (1996):2237–2244.
9. A. Marrocchi, L. Minuti, G. Morozzi, L. Pampanella, and A. Taticchi, Synthesis and mutagenicity of some cyclopenta[*c*]phenanthrenes and indeno[*c*]phenanthrenes. *Carcinogenesis* 17 (1996):2009–2012.
10. J. J. Sepiol, M. Gora, and M. K. Luczynski, Synthesis of cycloalka[*a*]- and cycloalka [*c*]phenanthrene aminonitriles from 2-(1-naphthyl)cycloalkylidene malonodinitriles involving novel aromatic rearrangement. *Synlett* 9 (2001):1383–1386.
11. E. Gacs-Baitz, L. Minuti, and A. Taticchi, A new short synthetic approach to cyclopentaphenanthrenones. *Tetrahedron* 50 (1994):10359–10366.
12. A. Altomare, G. Cascarano, C. Giacovazzo, and A. Guagliardi, SIR92—A program for crystal structure solution. *J. Appl. Crystallogr.* 26 (1993):343–350.
13. G. M. Sheldrick, SHELXSL-97. Program for crystal structure refinement. Germany: University of Goettingen (1997).
14. E. F. Prentice, T. A. Flagg, C. A. McCutcheon, D. F. Brastow, and D. C. Cross, Equipement, methods, and automated data-entry station for PIT tagging. *Am. Fish Soc. Symp.* 7 (1990):335–340.
15. K. R. Carrasco, K. L. Tilbury, and M. S. Myers, Assessment of the piscine micronucleus test as an *in situ* biological indicator of chemical contaminant effects. *Can. J. Fish Aquat. Sci.* 47 (1990):2123–2136.
16. P. Woźnicki, R. Lewandowska, P. Brzuzan, E. Ziomek, and R. Bardega, The level of DNA damage and the frequency of micronuclei in haemolymph of freshwater mussels *Anodonta woodiana* exposed to benzo[*a*]pyrene. *Acta Toxicologica*, 12 (2004):41–45.
17. C. M. Gedik, S. W. Ewen, and A. R. Colins, Single cell gel electrophoresis applied to the analysis of UV-C damage and its repair in human cells. *Int. J. Radiat. Biol.* 62 (1992):313–320.
18. G. H. S. Strauss, Non-random cell effects. *Mutat. Res.* 252 (1991):1–15.
19. C. B. Rees, S. D. McCormick, J. P. Vanden Heuvel, and W. Li, Quantitative PCR analysis of CYP1A induction in Atlantic salmon (*Salmo salar*). *Aquat. Toxicol.* 62 (2003):67–78.
20. R. G. Miller, Simultaneous statistical inference. 2 ed. New York: Springer-Verlag (1981).
21. L. J. Farrugia, WinGX suite for small-molecule single-crystal crystallography. *J. Appl. Cryst.* 32 (1999):837–838.

22. J. Bernstein, H. Regev, and F. H. Herbstein, Molecular compounds and complexes. X. The crystal structure of the -molecular compound benzo[*c*]phenanthrene-2,3-dichloro-5,6-dicyanobenzoquinone. *Acta Crystallogr., Sect.B: Struct. Crystallogr. Cryst. Chem.* 33 (1977):1716–1724.
23. F. L. Hirshfeld, S. Sandler, and G. M. J. Schmidt, The structure of overcrowded aromatic compounds. VI. The crystal structure of benzo[*c*]phenanthrene and of 1,12-dimethylbenzo[*c*]phenanthrene. *J. Chem. Soc.* (1963), 2108–2125.
24. P. L. Lakshman, S. Kole, J. H. Chaturvedi, H. J. Saugier, C. Yeh, J. P. Glusker, H. L. Carrell, A. K. Katz, C. E. Afshar, W.-M. Dashwood, G. Kenniston, and W. M. Baird, Methyl Group-Induced Helicity in 1,4-Dimethylbenzo[*c*]phenanthrene and Its Metabolites: Synthesis, Physical, and Biological Properties. *J. Am. Chem. Soc.* 122 (2000):12629–12636.
25. M. J. Musmar, G. E. Martin, R. T. Gampe Jr., V. M. Lynch, S. H. Simonsen, M. L. Lee, M. L. Tedjamulia, and R. N. Castle, 1-Methylphenanthro[3,4-*b*]thiophene: determination of the tertiary structure in solution and in the crystalline state by NMR spectroscopy and X-ray diffraction. *J. Heterocycl.Chem*. 22 (1985): 545.
26. R. E. Gerkin, Hydrogen bonding and C-H$\cdots$O interactions in 4-phenanthrenemethanol at 150°K . *Acta Crystallogr., Sect.C: Cryst. Struct. Commun.* 56 (2000): 1287–1288.
27. L. Shimoni, H. L. Carrell, J. P. Glusker, and M. M. Coombs, Intermolecular effects in crystals of 11-(trifluoromethyl)-15,16-dihydrocyclopenta[*a*]phenanthren-17-one. *J. Am. Chem. Soc.* 116 (1994):8162–8168.
28. S. T. Hadfield, T. S. Bhatt, and M. M Coombs, The biological activity and activation of 15,16-dihydro-1,11-methanocyclopenta[*a*]phenanthren-17-one, a carcinogen with obstructed bay region. *Carcinogenesis* 5 (1984):1485–1491.
29. M. E. Hahn, R. R. Merson, and S. I. Karchner, Xenobiotic receptors in fish: Structural and functional diversity and evolutionary insights. In: Moon, T. W. and Mommsen, T. P., (eds.), *Biochemical and Molecular Biology of Fishes Volume 6 Environmental Toxicology*. New York: Elsevier pp. 191–228 (2005).
30. A. Solhaug, M. Refsnes, M. Låg, P. E. Schwarze, T. Husøy, and J. A. Holme, Polycyclic aromatic hydrocarbons induce both apoptotic and anti-apoptotic signals in Hepa1c1c7 cells**.** *Carcinogenesis* 25 (2004):809–819.
31. N. M. Johnsen, S. H. Nyholm, K. Haug, T. Scholz, and J. A. Holme, Metabolism and activation of cyclopenta polycyclic aromatic hydrocarbons in liver tissue from rats and humans. *Chem. Biol. Interact.* 113 (1998):217–237.
32. H.-F. Chang, D. M. Huffer, P. Chiarelli, L. R. Blankenship, S. J. Culp, and B. P. Cho, Characterization of DNA Adducts Derived from syn-Benzo[*ghi*]fluoranthene-3,4-Dihydrodiol-5,5a-Epoxide and Comparative DNA Binding Studies with Structurally-Related anti-Diolepoxides of Benzo[*ghi*]fluoranthene and Benzo[*c*]-phenanthrene *Chem. Res. Toxicol.* 15 (2002):198–208.
33. M. K. Luczyński, M. Góra, P. Brzuzan, J. Wilamowski, and B. Kozik, Oxidative metabolism, mutagenic and carcinogenic properties of some polycyclic aromatic hydrocarbons *Env. Biotech.* 1 (2005):16–28.
34. D. S. Vienneau, U. DeBoni, and P. G Wells, Potential genoprotective role for UDP-glucuronosyltransferases in chemical carcinogenesis: initiation of micronuclei by

benzo[a]pyrene and benzo[e]pyrene in UDP-glucuronosyltransferase-deficient cultured rat skin fibroblasts. *Cancer Res.* 55 (1995):1045–1051.

35. K. Al-Sabti, and C. D. Metcalfe, Fish micronuclei for assessing genotoxicity in water. *Mut. Res*. 343 (1995):121–135.
36. A. Ramesh, F. Inyang, D. B. Hood, and M. E. Knuckles, Aryl hydrocarbon hydroxylase activity in F-344 rats subchronically exposed to benzo[*a*]pyrene and fluoranthene through diet. *J. Biochem. Molecular Toxicology* 14 (2000):155–161.
37. J. Wu, A. Ramesh, T. Nayyar, and D. B. Hood, Assessment of metabolites and AhR and CYP1A1 mRNA expression subsequent to prenatal exposure to inhaled benzo[*a*]pyrene. *Int. J. Dev. Neurosci*. 21 (2003):333–346.